Acta Cryst. (1998). B**54**, 722–731

Ideal and Real Structure of $Ti_5O_4(PO_4)_4$: X-ray and HRTEM Investigations†

Felix Reinauer and Robert Glaum*

Institut für Anorganische und Analytische Chemie der Justus-Liebig-Universität, Heinrich Buff-Ring 58, D-35392 Giessen, Germany. E-mail: robert.glaum@anorg.chemie.uni-giessen.de

(*Received 1 December 1997; accepted 2 March 1998*)

Abstract

The crystal structure of pentatitanium tetraoxide tetrakis(phosphate), $Ti_5O_4(PO_4)_4$, has been determined and refined from X-ray diffraction single-crystal data [$P2_12_12_1$ (No. 19), Z = 4, a = 12.8417 (12), b = 14.4195 (13), c = 7.4622 (9) Å (from Guinier photographs); conventional residual R_1 = 0.042 for 2556 $F_o > 4\sigma(F_o)$, R_1 = 0.057 for all 3276 independent reflections; 282 parameters; 29 atoms in the asymmetric unit of the ideal structure]. The structure is closely related to those of β-$Fe_2O(PO_4)$-type phosphates and synthetic lipscombite, $Fe_3(PO_4)_4(OH)$. While these consist of infinite chains of face-sharing MO_6 octahedra, in pentatitanium tetraoxide tetrakis(phosphate) only five-eighths of the octahedral voids are occupied according to $\square_3Ti_5O_4(PO_4)_4$. Four of the five independent $Ti^{4+}O_6$ show high radial distortion [$1.72 \leq d(\mathrm{Ti-O}) \leq 2.39$ Å] and a typical 1 + 4 + 1 distance distribution. The fifth $Ti^{4+}O_6$ is an almost regular octahedron [$1.91 \leq d(\mathrm{Ti-O}) \leq 1.98$ Å]. Partial disorder of Ti^{4+} over the available octahedral voids is revealed by the X-ray structure refinement. High-resolution transmission electron microscopy (HRTEM) investigations confirm this result.

1. Introduction

The remarkable optical properties of potassium titanyl phosphate, $KTiOPO_4$, KTP (Tordjman *et al.*, 1974; Stucky *et al.*, 1988), with its high non-linear optical coefficient, as well as the high ionic conductivity of NASICON-type phosphates such as $NaM_2(PO_4)_3$ (M = Ge^{4+}, Ti^{4+}, Zr^{4+}; Hagman & Kierkegaard, 1968), have led to a growing interest in titanium(IV) phosphates. Numerous ongoing investigations are dealing with the synthesis, crystal chemistry and physical properties of members of this class of compound. Despite this, the crystal structure of $Ti_5O_4(PO_4)_4$ is still not well established.

Early investigations on the pseudo-binary system TiO_2/P_2O_5 (Harrison & Hummel, 1959; Golynko-Vol'fson & Sudakas, 1966) led to the assumption of two additional titanium(IV) phosphates, $Ti_2P_2O_9$ and $Ti_5P_4O_{20}$, besides the long-known diphosphate TiP_2O_7 (Levi & Peyronel, 1935). From further investigations it has been concluded that there should be only one additional phosphate to which the formula $Ti_2P_2O_9$ has been ascribed (Bamberger & Begun, 1987). In a paper on phase relations and crystal growth by chemical vapour transport in the pseudo-ternary system $TiO_2/TiP_2O_7/TiPO_4$ (Reinauer *et al.*, 1994) we have confirmed the existence of $Ti_5P_4O_{20}$ as the only titanium(IV) phosphate besides TiP_2O_7. For structural reasons we prefer the formula $Ti_5O_4(PO_4)_4$ rather than $Ti_5P_4O_{20}$.

In this paper we report the results of a combined X-ray single-crystal and HRTEM investigation of $Ti_5O_4(PO_4)_4$.

2. Experimental

2.1. *Synthesis*

Pentatitanium tetraoxide tetrakis(phosphate) can be synthesized following (1). By reacting stoichiometric mixtures of TiO_2 (Merck) and TiP_2O_7 (Winkler & Thilo, 1966) in evacuated silica ampoules with Cl_2 as the mineralizer at 1173 K for 14 d very light pink crystals with edge length up to 0.2 mm were obtained. They were generally of square-bipyramidal shape.

$$3TiO_{2,s} + 2TiP_2O_{7,s} \rightarrow Ti_5O_4(PO_4)_{4,s} \qquad (1)$$

Crystallization of $Ti_5O_4(PO_4)_4$ can also be accomplished by chemical vapour transport (1273 → 1173 K; 1 atm. Cl_2 + 5 mg $TiPO_4$ as the transport agent) with migration rates $\dot{m} \simeq 1$ mg d^{-1}, as has been reported earlier (Reinauer *et al.*, 1994). Thus, transparent crystals of pale amber colour with edge length up to 0.12 mm and rectangular shape were obtained.

X-ray fluorescence (EDX) analyses of selected crystals gave a Ti:P ratio of 1.16 [theoretical value for $Ti_5O_4(PO_4)_4$ = 1.25]. No hints of other elements, especially silicon, were found (Table 1).

2.2. *X-ray investigations*

Crystals for structural investigations were selected under polarized light and were checked for perfect

† This is part XX of a series on the thermal behaviour and crystal chemistry of anhydrous phosphates. For part XIX see Glaum & Schmidt (1997). This paper is part of the PhD thesis of Reinauer (1998).

Table 1. *Atomic ratio Ti:P from EDX analyses of different crystals of* $Ti_5O_4(PO_4)_4$

Crystal	Ti:P
1	1.15
2	1.18
3	1.17
Average	1.16
$Ti_5O_4(PO_4)_4$	1.25

extinction. X-ray single-crystal photographs show only serial extinctions ($h00 \neq 2n$; $0k0 \neq 2n$; $00l \neq 2n$), indicating the orthorhombic space group $P2_12_12_1$. We attribute the occurrence of these reflections in the electron diffraction pattern of the [001] zone (Fig. 1) to 'multiple diffraction' (German: *Umweganregung*; Renninger, 1935). This effect is well known in electron diffraction and far more important than in X-ray crystallography for intensity enhancement of reflections otherwise forbidden by symmetry. Cell parameters from X-ray investigations (Table 2) and electron diffraction (Figs. 1 and 2) are in agreement. A crystal of rectangular shape (0.11 × 0.09 × 0.05 mm) from a chemical vapour transport experiment has been used for the intensity measurement with an imaging plate diffraction system (IPDS) (Fa. Stoe & Cie). Details of intensity measurement and structure refinement are given in Table 2. A numerical absorption correction has been applied with the program *SHELX*76 (Sheldrick, 1976) on the basis of the optimized crystal shape. After preliminary inspection of the crystal under a stereo-microscope, crystal faces and distances have been optimized by minimizing the internal R value of symmetry-equivalent and other multiply measured (IPDS technique) reflections using the program *HABITUS* (Herrendorf, 1993). Attempts to solve the structure by direct methods with *SHELXS*86 (Sheldrick, 1985) led to a combined figure-of-merit CFOM = 0.02. Starting with only four titanium positions, the structure model could be refined in the non-centrosymmetric space group $P2_12_12_1$ using *SHELXL*93 (Sheldrick, 1993). Allowance for racemic twinning has been given in the refinement according to a method described by Bernardinelli & Flack (1985). Missing Ti, P and O atoms were located from successive difference Fourier syntheses. However, the 'anisotropic' refinement converged rather slowly and locating all the missing atoms from difference Fourier syntheses turned out to be very difficult. Eventually, with all atoms included, according to $Ti_5O_4(PO_4)_4$, only a rather poor conventional residual $R_1 = 0.12$ ($wR_2 = 0.24$ on F^2; $S = 1.82$) could be obtained with three maxima (~7.5 e Å^{-3}) remaining in the residual electron density map. Some atoms also showed non-positive definite displacement parameters at this stage of refinement [model (I)].

Initial attempts to explain the residual electron density by twinning failed. Refinements in space groups with lower symmetry were unsuccessful as well as those in higher symmetry space groups (trigonal, hexagonal) implied by the axial ratio $a/c \simeq 3^{1/2}$. Eventually we tried refinement of the structure allowing for disorder of the Ti atoms [model (II)]. This model has been assumed because all three highest maxima in the difference Fourier map showed an environment of six O atoms already present in the ideal structure, with chemically reasonable Ti—O distances from 1.8 to 2.4 Å. In model (II) 20 Ti atoms are spread over eight fourfold sites (five

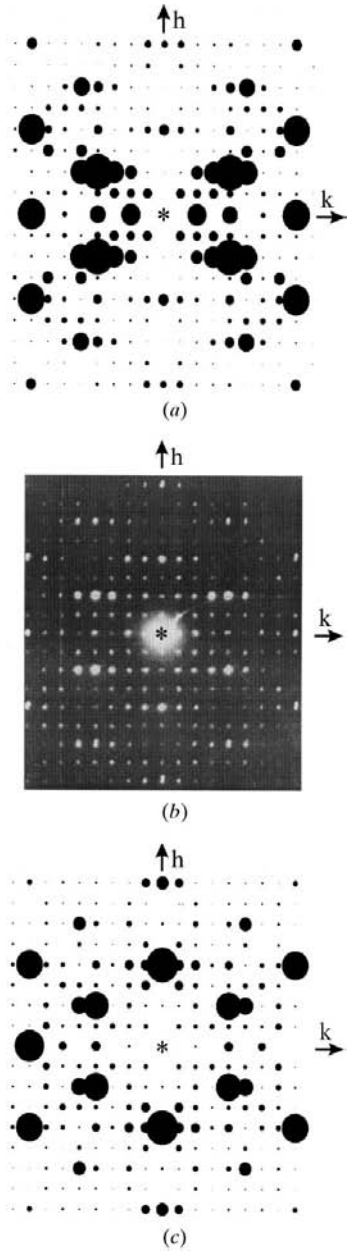

Fig. 1. Electron diffraction pattern of $Ti_5O_4(PO_4)_4$ along [001]. (*a*) Simulation using the ideal structure [model (I)]; (*b*) observed electron diffraction pattern; (*c*) simulation using the data from X-ray structure refinement [model (II)].

original positions; three positions from the difference Fourier map). Isotropic displacement parameters for the additional titanium sites were constrained to be equal in the final calculation. Refinement of Ti6, Ti7 and Ti8 with one isotropic displacement parameter constrained to the average U_{eq} of Ti1–Ti5 did not significantly change the s.o.f.'s (site occupancy factors) for these sites (0.073, 0.150 and 0.129 rather than 0.063, 0.135 and 0.113). Additionally, in these calculations a total of 20 Ti atoms were restrained (*SUMP* option in *SHELXL*93) to be located on $8 \times 4 = 32$ positions. This led to $R_1 = 0.057$, $wR_2 = 0.143$ and a goodness-of-fit $S = 1.11$ (for all reflections). The residual electron density was reduced to 0.68 e Å^{-3}. The refinement yielded an s.o.f. $\simeq 0.9$ for Ti1, Ti2 and Ti3. Within the error limits of the determination the Ti4 and Ti5 sites were fully occupied. For the additional sites Ti6, Ti7 and Ti8 in model (II),

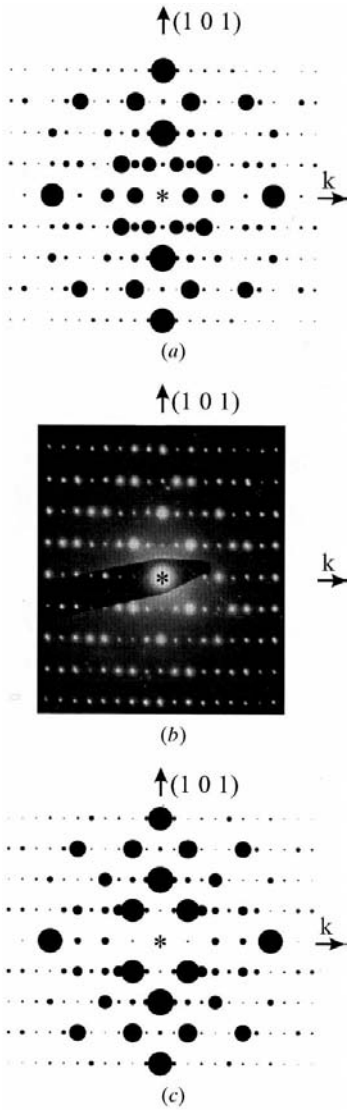

Fig. 2. Electron diffraction pattern of $Ti_5O_4(PO_4)_4$ along $[10\bar{1}]$. (*a*) Simulation using the ideal structure [model (I)]; (*b*) observed electron diffraction pattern; (*c*) simulation using the data from X-ray structure refinement [model (II)].

Table 2. *Experimental details*

Crystal data	
Chemical formula	$Ti_5O_4(PO_4)_4$
Chemical formula weight	683.38
Cell setting	Orthorhombic
Space group	$P2_12_12_1$
a (Å)	12.8417 (12)
b (Å)	14.4195 (13)
c (Å)	7.4622 (9)
V (Å^3)	1381.8 (2)
Z	4
D_x (Mg m^{-3})	3.285
Radiation type	Mo $K\alpha$
Wavelength (Å)	0.71069
No. of reflections for cell parameters	25
θ range (°)	6.98–31.48
μ (mm^{-1})	3.355
Temperature (K)	293 (2)
Crystal form	Rectangular
Crystal size (mm)	0.11 × 0.09 × 0.05
Crystal colour	Transparent pale amber
Data collection	
Diffractometer	Imaging plate diffraction system, Fa. Stoe & Cie
Data collection method	Area detector scans
Absorption correction	Numerical
T_{min}	0.365
T_{max}	0.680
No. of measured reflections	10 334
No. of independent reflections	3276
No. of observed reflections	2556
Criterion for observed reflections	$I > 2\sigma(I)$
R_{int}	0.0860
θ_{max} (°)	27.99
Range of h, k, l	$-16 \rightarrow h \rightarrow 16$ $-18 \rightarrow k \rightarrow 18$ $-9 \rightarrow l \rightarrow 9$
Refinement	
Refinement on	F^2
$R[F^2 > 2\sigma(F^2)]$	0.0418
$wR(F^2)$	0.1364
S	1.213
No. of reflections used in refinement	3276
No. of parameters used	282
Weighting scheme	$w = 1/[\sigma^2(F_o^2) + (0.0753P)^2]$, where $P = (F_o^2 + 2F_c^2)/3$
$(\Delta/\sigma)_{max}$	−0.003
$\Delta\rho_{max}$ (e Å^{-3})	0.683
$\Delta\rho_{min}$ (e Å^{-3})	−0.743
Extinction method	*SHELXL*93 (Sheldrick, 1993)
Extinction coefficient	0.0005 (7)
Source of atomic scattering factors	*International Tables for Crystallography* (1992, Vol. C, Tables 4.2.6.8 and 6.1.1.4)
Computer programs	
Structure solution	*SHELXS*86 (Sheldrick, 1990)
Structure refinement	*SHELXL*93 (Sheldrick, 1993)

Table 3. *Fractional atomic coordinates and equivalent isotropic displacement parameters (Å²)*

$U_{eq} = (1/3)\Sigma_i\Sigma_j U^{ij} a^i a^j \mathbf{a}_i.\mathbf{a}_j$.

	x	*y*	*z*	s.o.f.	U_{eq}
Ti1	0.85634 (12)	0.67658 (10)	0.8929 (2)	0.901 (6)	0.0080 (4)
Ti2	0.36442 (13)	0.67261 (12)	0.4014 (2)	0.869 (6)	0.0093 (4)
Ti3	0.39273 (12)	0.20588 (10)	0.3491 (2)	0.895 (6)	0.0081 (4)
Ti4	0.11466 (12)	0.94697 (10)	0.1463 (2)	1.023 (6)	0.0127 (4)
Ti5	0.6230 (2)	0.94120 (13)	0.6250 (3)	0.997 (5)	0.0162 (4)
Ti6	0.6424 (12)	0.4226 (12)	0.5962 (21)	0.063 (4)	0.002 (2)
Ti7	0.8936 (7)	0.2060 (6)	0.8471 (12)	0.135 (5)	0.002 (2)
Ti8	0.3627 (7)	0.5782 (7)	0.6011 (12)	0.113 (4)	0.002 (2)
P1	0.00327 (12)	−0.00008 (10)	0.7612 (5)	1	0.0072 (5)
P2	0.4911 (2)	0.75269 (10)	0.7575 (2)	1	0.0067 (5)
P3	0.7555 (2)	0.12225 (12)	0.4837 (4)	1	0.0078 (5)
P4	0.7541 (2)	0.37348 (12)	0.0021 (4)	1	0.0080 (5)
O1	0.0108 (5)	0.2560 (3)	0.7354 (7)	1	0.0156 (15)
O2	0.0013 (4)	0.4973 (3)	0.2863 (12)	1	0.018 (2)
O3	0.2507 (4)	0.3786 (3)	0.9660 (11)	1	0.0153 (15)
O4	0.2621 (5)	0.1353 (4)	0.5330 (10)	1	0.0176 (13)
O11	0.4393 (5)	0.5599 (4)	0.3630 (11)	1	0.0174 (14)
O12	0.9237 (5)	0.5627 (4)	0.8434 (11)	1	0.0181 (14)
O13	0.4320 (5)	0.4434 (4)	0.1170 (10)	1	0.0178 (14)
O14	0.5730 (5)	0.5654 (4)	0.1218 (9)	1	0.0127 (13)
O21	0.5641 (5)	0.8184 (5)	0.6603 (10)	1	0.0193 (15)
O22	0.0822 (5)	0.1943 (5)	0.3808 (10)	1	0.0178 (13)
O23	0.0700 (5)	0.3038 (5)	0.1245 (10)	1	0.0185 (14)
O24	0.0574 (5)	0.8118 (4)	0.1223 (10)	1	0.0138 (12)
O31	0.6857 (5)	0.0625 (4)	0.5980 (11)	1	0.0171 (14)
O32	0.8202 (5)	0.0608 (4)	0.3617 (9)	1	0.0128 (13)
O33	0.8270 (5)	0.1812 (4)	0.5982 (10)	1	0.0155 (14)
O34	0.3120 (5)	0.6879 (4)	0.1350 (9)	1	0.0130 (12)
O41	0.8289 (5)	0.4250 (4)	0.1260 (9)	1	0.0162 (13)
O42	0.3168 (5)	0.1828 (5)	0.1326 (11)	1	0.0189 (14)
O43	0.8135 (5)	0.6922 (4)	0.6201 (10)	1	0.0116 (12)
O44	0.8145 (5)	0.5570 (4)	0.4046 (11)	1	0.0187 (15)

Site occupancy factors (s.o.f.'s) of the Ti atoms have been calculated using the constraint of a total of 20 Ti atoms per unit cell (*SUMP* option in *SHELXL*93; Sheldrick, 1993). In addition, U_{eq} for Ti6, Ti7 amd Ti8 were forced to be equal.

compared with the ideal structure with no disorder [model (I)], occupation factors of 0.063 (4), 0.135 (5) and 0.114 (4), respectively, were obtained.†

The X-ray Guinier powder pattern of $Ti_5O_4(PO_4)_4$ is in good agreement with the pattern calculated on the basis of the structural parameters derived from the single-crystal data. Relevant experimental and crystallographic data for $Ti_5O_4(PO_4)_4$ are given in Table 2, final atomic parameters in Table 3 and distances within the TiO_6 and PO_4 polyhedra in Table 4. The numbering scheme used for oxygen throughout the paper distinguishes between 'oxidic' oxygen (O1–O4) and 'phosphate' oxygen (O11–O44), where the first digit refers to the corresponding P atom.

2.3. *Structure description*

The crystal structure of $Ti_5O_4(PO_4)_4$ is closely related to that of a series of isotypic oxide phosphates $M_2O(PO_4)$ ($I4_1/amd$, $Z = 4$, $a \simeq 5.3$, $c \simeq 12.8$ Å), including β-$Fe_2O(PO_4)$ (Ijjaali *et al.*, 1990), $NiCrO(PO_4)$ (Ech-Chahed *et al.*, 1988) and β-$V_2O(PO_4)$ (Glaum & Gruehn, 1989). Synthetic lipscombite, $Fe_3(PO_4)_2(OH)_2$ ($I4_32_12$, $Z = 4$, $a \simeq 7.3$, $c \simeq 13.2$ Å; Vencato *et al.*, 1989), also belongs to this structure family. The metric relationship of pentatitanium tetraoxide tetrakis(phosphate) to β-$Fe_2O(PO_4)$ is given by the matrix $a' = c$, $b' = 2a + 2b$, $c' = a - b$, where a', b' and c' denote the axes of $Ti_5O_4(PO_4)_4$, while a, b and c represent those of the β-$Fe_2O(PO_4)$ structure type. The symmetry relation in terms of group/subgroup considerations (Bärnighausen, 1980) is described in Fig. 3.

Characteristic structural features of the aristotype [β-$Fe_2O(PO_4)$ structure] are infinite chains built by face-sharing MO_6 octahedra. Series of perpendicular chains are linked *via* common (oxidic) O atoms (Fig. 4*a*). Coordination by four equidistant $M^{2+/3+}$ is observed for these O atoms. In the completely ordered ideal structure of $Ti_5O_4(PO_4)_4$ [model (I)] three-eighths of the octahedral voids are empty, in order to keep the charge balance (20 Ti^{4+} on 32 positions rather than 16 Fe^{2+} and 16 Fe^{3+}

† Supplementary data for this paper are available from the IUCr electronic archives (Reference: JZ0005). Services for accessing these data are described at the back of the journal.

Table 4. *Interatomic distances (Å) and bond angles (°) in $Ti_5O_4(PO_4)_4$*

Bond distances d(Ti—O) and d(P—O) are shown in bold; d(O—O) in the upper right, ∠(O, X, O) in the lower left part of a data block. S.u.'s are given in parentheses.

Ti1	O4^{i}	O22^{i}	O12	O34^{ii}	O43	O1^{i}
O4^{i}	**1.725 (6)**	2.712 (9)	2.765 (9)	2.826 (9)	2.884 (10)	3.966 (11)
O22^{i}	97.4 (3)	**1.883 (7)**	2.800 (11)	2.886 (8)	3.958 (11)	2.938 (9)
O12	99.6 (3)	95.8 (3)	**1.892 (6)**	3.875 (10)	2.876 (9)	2.970 (8)
O34^{ii}	96.7 (3)	94.5 (3)	159.4 (3)	**2.044 (6)**	2.515 (12)	2.529 (9)
O43	96.6 (3)	162.9 (3)	91.4 (3)	74.3 (3)	**2.122 (7)**	2.664 (9)
O1^{i}	166.8 (2)	89.7 (3)	90.7 (3)	71.6 (2)	74.7 (2)	**2.266 (6)**
Ti2	O3^{iii}	O23^{iv}	O11	O43^{v}	O34	O1^{iii}
O3^{iii}	**1.721 (6)**	2.819 (9)	2.707 (9)	2.884 (8)	2.769 (9)	3.947 (11)
O23^{iv}	102.3 (3)	**1.897 (8)**	2.773 (11)	2.856 (8)	3.956 (11)	3.080 (9)
O11	96.3 (3)	93.5 (3)	**1.909 (6)**	3.925 (10)	2.997 (9)	2.893 (8)
O43^{v}	98.9 (2)	92.2 (3)	162.2 (3)	**2.061 (6)**	2.515 (12)	2.664 (9)
O34	92.0 (3)	161.8 (3)	96.2 (3)	74.1 (3)	**2.112 (7)**	2.529 (9)
O1^{iii}	162.3 (2)	94.8 (3)	87.0 (3)	75.7 (2)	70.4 (2)	**2.272 (6)**
Ti3	O1^{vi}	O33^{vii}	O42	O14^{viii}	O24^{iv}	O4
O1^{vi}	**1.732 (7)**	2.789 (9)	2.821 (9)	2.917 (8)	2.922 (9)	4.083 (12)
O33^{vii}	101.2 (3)	**1.875 (6)**	2.811 (12)	3.877 (9)	2.908 (8)	2.942 (9)
O42	101.2 (3)	95.7 (3)	**1.917 (7)**	2.868 (8)	3.996 (11)	3.145 (10)
O14^{viii}	99.3 (3)	156.5 (3)	91.5 (3)	**2.083 (6)**	2.548 (10)	2.614 (9)
O24^{iv}	97.0 (2)	92.2 (3)	158.4 (3)	74.0 (3)	**2.153 (7)**	2.530 (9)
O4	163.1 (2)	86.2 (3)	93.0 (3)	71.0 (2)	67.4 (2)	**2.394 (7)**
Ti4	O2^{ix}	O44^{x}	O41^{x}	O14^{xi}	O24	O4^{iii}
O2^{ix}	**1.731 (5)**	2.697 (8)	2.724 (8)	2.827 (9)	2.862 (8)	3.861 (7)
O44^{x}	97.0 (3)	**1.868 (6)**	2.825 (9)	2.798 (7)	3.906 (8)	2.891 (9)
O41^{x}	98.0 (3)	98.0 (3)	**1.876 (7)**	3.911 (9)	2.886 (7)	2.823 (8)
O14^{xi}	95.4 (3)	90.2 (3)	163.3 (3)	**2.079 (7)**	2.548 (10)	2.614 (9)
O24	96.5 (2)	161.1 (3)	93.2 (3)	75.4 (3)	**2.090 (6)**	2.530 (9)
O4^{iii}	168.0 (3)	91.7 (3)	88.8 (3)	76.3 (3)	73.2 (2)	**2.150 (6)**
Ti5	O32^{xii}	O2^{ii}	O31^{xiii}	O13^{x}	O21	O3^{i}
O32^{xii}	**1.912 (7)**	2.704 (8)	2.653 (9)	3.850 (12)	2.739 (9)	2.746 (8)
O2^{ii}	90.0 (3)	**1.915 (6)**	2.664 (8)	2.749 (9)	2.806 (8)	3.891 (7)
O31^{xiii}	87.2 (3)	87.5 (2)	**1.934 (6)**	2.794 (9)	3.878 (7)	2.814 (8)
O13^{x}	178.9 (4)	91.0 (3)	92.3 (3)	**1.941 (8)**	2.744 (11)	2.750 (9)
O21	90.6 (3)	93.3 (2)	177.6 (4)	89.9 (3)	**1.943 (7)**	2.702 (9)
O3^{i}	89.9 (3)	179.5 (4)	92.0 (3)	89.2 (3)	87.1 (3)	**1.976 (6)**
P1	O11^{vii}	O12^{xiv}	O13^{vii}	O14^{vii}		
O11^{vii}	**1.509 (7)**	2.497 (8)	2.490 (11)	2.489 (9)		
O12^{xiv}	111.2 (4)	**1.519 (7)**	2.509 (9)	2.480 (8)		
O13^{vii}	110.2 (5)	110.9 (3)	**1.528 (7)**	2.526 (8)		
O14^{vii}	108.1 (3)	107.0 (5)	109.4 (3)	**1.566 (6)**		
P2	O23^{iv}	O21	O22^{iv}	O24^{ii}		
O23^{iv}	**1.505 (7)**	2.478 (13)	2.485 (9)	2.502 (8)		
O21	110.1 (5)	**1.517 (7)**	2.504 (10)	2.482 (8)		
O22^{iv}	110.4 (4)	110.9 (4)	**1.522 (7)**	2.466 (13)		
O24^{ii}	110.1 (3)	108.2 (3)	107.0 (5)	**1.546 (7)**		
P3	O31	O33	O32	O34^{viii}		
O31	**1.508 (7)**	2.496 (9)	2.469 (9)	2.510 (11)		
O33	111.2 (4)	**1.515 (7)**	2.476 (9)	2.495 (8)		
O32	109.3 (3)	109.5 (4)	**1.518 (6)**	2.499 (9)		
O34^{viii}	109.8 (4)	108.4 (3)	108.6 (4)	**1.560 (7)**		
P4	O44^{xv}	O42^{xvi}	O41	O43^{xv}		
O44^{xv}	**1.520 (7)**	2.492 (10)	2.488 (9)	2.527 (10)		
O42^{xvi}	110.0 (4)	**1.523 (7)**	2.483 (11)	2.525 (8)		
O41	109.5 (4)	109.0 (4)	**1.526 (6)**	2.491 (9)		
O43^{xv}	110.4 (4)	110.1 (3)	107.8 (4)	**1.557 (6)**		

Symmetry codes: (i) $-x+1, y+\frac{1}{2}, -z+\frac{3}{2}$; (ii) $x+\frac{1}{2}, -y+\frac{3}{2}, -z+1$; (iii) $-x+\frac{1}{2}, -y+1, z-\frac{1}{2}$; (iv) $-x+\frac{1}{2}, -y+1, z+\frac{1}{2}$; (v) $x-\frac{1}{2}, -y+\frac{3}{2}, -z+1$; (vi) $x+\frac{1}{2}, -y+\frac{1}{2}, -z+1$; (vii) $x-\frac{1}{2}, -y+\frac{1}{2}, -z+1$; (viii) $-x+1, y-\frac{1}{2}, -z+\frac{1}{2}$; (ix) $-x, y+\frac{1}{2}, -z+\frac{1}{2}$; (x) $-x+1, y+\frac{1}{2}, -z+\frac{1}{2}$; (xi) $x-\frac{1}{2}, -y+\frac{3}{2}, -z$; (xii) $-x+\frac{3}{2}, -y+1, z+\frac{1}{2}$; (xiii) $x, y+1, z$; (xiv) $-x+1, y-\frac{1}{2}, -z+\frac{3}{2}$; (xv) $-x+\frac{3}{2}, -y+1, z-\frac{1}{2}$; (xvi) $x+\frac{1}{2}, -y+\frac{1}{2}, -z$.

on 32 positions). This is expressed by the formula $\square_3Ti_5O_4(PO_4)_4$. A sequence ...*EOOEOOEOE*... of empty '*E*' and occupied '*O*' octahedral voids is observed in the completely ordered structure of the titanium(IV) phosphate [model (I)]. In Fig. 4 the structures of β-$Fe_2O(PO_4)$ and $\square_3Ti_5O_4(PO_4)_4$ are compared.

The structure of pentatitanium tetraoxide tetrakis(phosphate) consists of four distorted TiO_6 octahedra (Ti1–Ti4) with d(Ti—O) ranging from 1.72 to 2.39 Å (Table 4). These octahedra share common faces, forming two Ti_2O_9 groups (Fig. 5). Distances d(Ti—O) > 2.04 Å from Ti to bridging O atoms and $1.72 \leq d(\text{Ti—O}) \leq 1.92$ Å to terminal O atoms in the dimers reflect the electrostatic repulsion between the highly charged Ti^{4+}. The fifth TiO_6, containing Ti5, is far less distorted with Ti—O distances ranging from 1.91 to 1.98 Å. Bond length–bond strength considerations (Brese & O'Keeffe, 1991) led to valence sums $v_{\text{Ti–O}}$ = 4.19, 4.07, 3.95, 4.34 and 4.32 for Ti1–Ti5, respectively (Table 5).

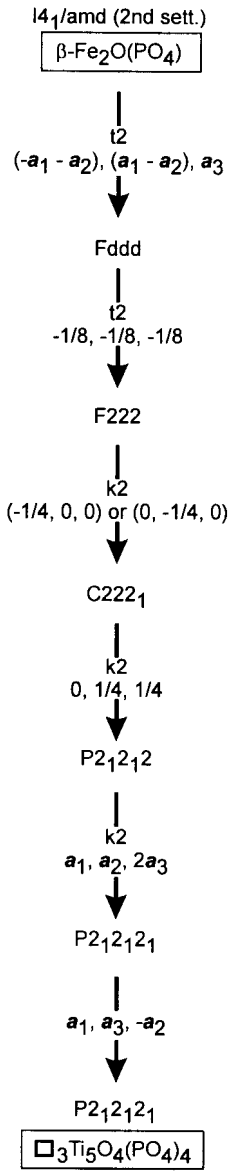

Fig. 3. Group–subgroup relationship between β-$Fe_2O(PO_4)$ and $Ti_5O_4(PO_4)_4$ structure types.

In contrast to the β-$Fe_2O(PO_4)$ structure with coordination number 4 for 'oxidic' oxygen, twofold (O2, O3) and threefold (O1, O4) coordination, respectively, is observed in titanium(IV) oxide phosphate owing to the lack of three-eighths of the Ti cations. The formation of one short bond [d(Ti—O) $\simeq$ 1.73 Å] compensates for this. O atoms of phosphate groups show either twofold (P + Ti) or threefold (P + 2Ti) coordination. It is observed that O atoms shortly bonded to P [$1.505 \leq d(\text{P—O}) \leq 1.528$ Å] are coordinated by only one Ti^{4+}, while those at a longer P—O distance ($d \geq 1.546$ Å) are bonded to two Ti atoms. Each PO_4 unit consists of three short and one long P—O bond. Each PO_4 tetrahedron is connected to four different Ti^{4+} cations. Projections of the $Ti_5O_4(PO_4)_4$ structure along [001] and [100] are shown in Fig. 6.

2.4. *HRTEM investigations*

The HRTEM specimens were prepared by crushing a few crystals in an agate mortar. The particles (~10 μm diameter) were transferred onto a perforated foil (carbon-coated Formvar) supported on a copper grid. The HRTEM studies were performed using a Philips CM30 electron microscope at 300 kV equipped with a double-tilt holder. Additional information on experimental parameters is summarized in Table 6.

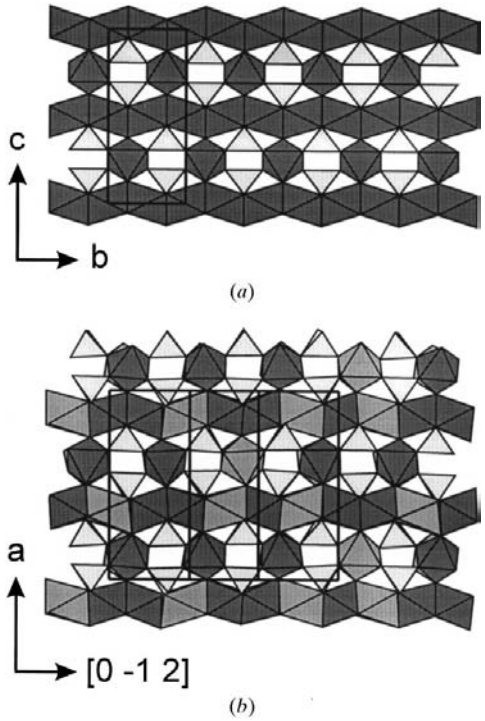

Fig. 4. Comparison between the structures of (*a*) β-$Fe_2O(PO_4)$ projected along [100] and (*b*) $Ti_5O_4(PO_4)_4$ projected on (021). Light grey: PO_4; dark grey: MO_6; medium grey: MO_6 not occupied in the ideal structure of $Ti_5O_4(PO_4)_4$. Plot produced with *ATOMS* (Dowty, 1995).

Table 5. *Bond strengths* v_{ij}

v_{ij} calculated according to $v_{ij} = \exp[(R_{ij} - d_{ij})/b]$ with $b = 0.37$ Å, $R_{ij}(Ti^{4+}-O^{2-}) = 1.815$ Å and $R_{ij}(P^{5+}-O^{2-}) = 1.604$ Å. Only sites occupied in the ideal structure are considered.

Atom	Ti1	Ti2	Ti3	Ti4	Ti5	P1	P2	P3	P4	v_{ij}
O1	0.296	0.291	1.251							1.838
O2				1.255	0.763					2.018
O3		1.289			0.647					1.936
O4	1.275		0.209	0.404						1.888
O11		0.721				1.293				2.014
O12	0.810					1.258				2.068
O13					0.713	1.228				1.941
O14			0.483	0.491		1.108				2.082
O21					0.706		1.265			1.971
O22	0.834						1.248			2.082
O23		0.803					1.307			2.110
O24			0.402	0.473			1.170			2.045
O31					0.723			1.296		2.019
O32					0.771			1.262		2.033
O33			0.848					1.272		2.120
O34	0.536	0.449						1.126		2.111
O41				0.850					1.235	2.085
O42			0.761						1.245	2.006
O43	0.439	0.513							1.135	2.087
O44				0.867					1.255	2.122
v_{ij}	4.190	4.066	3.954	4.340	4.323	4.887	4.990	4.956	4.870	

The investigations led to HRTEM images showing projections of the structure along [001] (Fig. 7) and [10$\bar{1}$] (Fig. 8). For both directions observed images and simulations on the basis of the X-ray data [model (I)] are in fairly good agreement. The simulations have been calculated near the Scherzer focus of −550 Å using the computer program *EMS* (Stadelmann, 1987). In particular, the contrast observed in the projection along [001] can be correlated easily with the crystal structure. Comparison of a projection of the TiO_6 octahedra of an array of four unit cells with a contrast simulation (Fig. 9) shows that the contrast is mainly determined by the Ti atoms. The simulation does not change much on varying the defocus from −350 to −750 Å. Dark parts of the HRTEM image can be attributed to titanium positions. Strings consisting of either three or five white spots belong to 'holes' between the TiO_6 polyhedra (Fig. 9). In the ideal structure a 'herringbone pattern' is formed by these strings. Observed and simulated contrast patterns for the projection along [001] match each other nicely (Fig. 7). However, on closer inspection of the HRTEM image of the [001] projection deviations from the ideal structure [model (I)] can be found.

Fig. 10(*a*) shows the magnification of an experimental image (projection along [001]) containing 4 × 4 unit cells. Deviations from the herringbone pattern are obvious. While the X-ray crystal structure refinement has given only an average picture of the disorder of the Ti^{4+} over the available octahedral voids, this HRTEM image shows the 'real' structure. In Fig. 10(*b*) a simu-

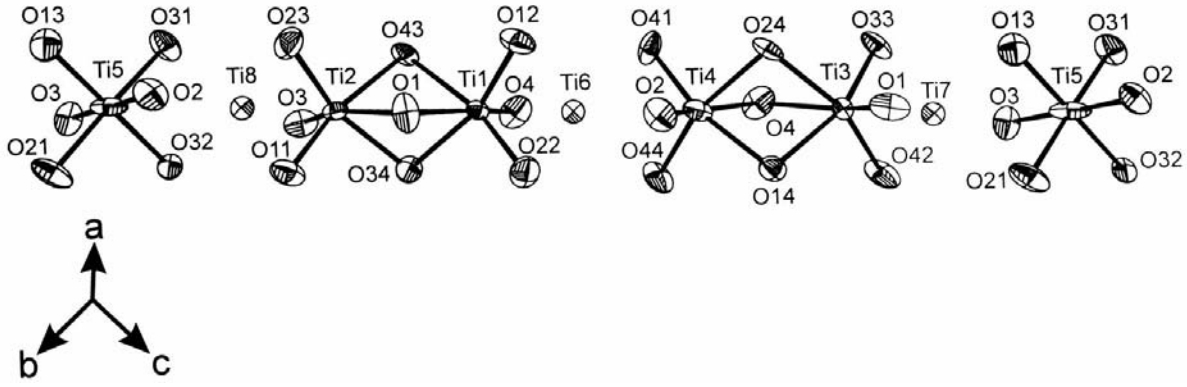

Fig. 5. *ORTEP* (Johnson, 1965) plot of a section of a 'chain' of face-sharing TiO_6 octahedra. Ellipsoids are shown at the 85% probability level. Ti6, Ti7 and Ti8 are shown as spheres with 0.5 Å radii.

lation (program *EMS*; Stadelmann, 1987) of this array of $4 \times 4 = 16$ unit cells is given, which matches the experimental image completely. The simulations were performed in the triclinic space group $P1$, keeping the positions of P and O from the X-ray refinement fixed. Just by distributing the Ti^{4+} over the octahedral sites according to the HRTEM image, coincidence between the experimentally observed and simulated contrast patterns could be obtained.

Table 6. *Parameters for contrast simulations of $Ti_5O_4(PO_4)_4$ with the program EMS (Stadelmann, 1987)*

Acceleration voltage (kV)	300
Objective lens aperture (nm^{-1})	10
Spherical aberation coefficient C_s (mm)	1.2
Spread of focus (nm)	10
Chromatic aberation (mrad)	0.8
Crystal thickness along [001] (nm)	3.7
Crystal thickness along [10$\bar{1}$] (nm)	4.5

3. Discussion

The crystal structure of pentatitanium tetraoxide tetrakis(phosphate), $Ti_5O_4(PO_4)_4$, was solved and refined from X-ray single-crystal data. The controversy regarding the composition of the second anhydrous titanium(IV) phosphate besides TiP_2O_7 is settled. The X-ray powder diffraction pattern reported some years ago (Bamberger & Begun, 1987) for '$(TiO)_2P_2O_7$' can be indexed completely on the basis of a two-phase mixture of $Ti_5O_4(PO_4)_4$ and TiP_2O_7. There is no evidence for a third titanium(IV) phosphate existing under equilibrium conditions.

The close structural relationship of $Ti_5O_4(PO_4)_4$ to the β-$Fe_2O(PO_4)$ structure type has been described in detail (see Figs. 3 and 4). It can be rationalized in terms of group–subgroup considerations. The relationship may be taken as a crystal-chemical explanation for the observed cation disordering with a distribution of 20 Ti^{4+} cations over 32 octahedral voids (eight fourfold sites) per unit cell. However, the distribution is not completely at random and a preference for Ti1–Ti5 sites of the ideal structure [model (I)] is still observed from X-ray single-crystal investigations and HRTEM studies.

Interatomic distances d(Ti—O) for $Ti1O_6$ to $Ti4O_6$ in $Ti_5O_4(PO_4)_4$ are very similar to those observed for $TiOSO_4$ (Gatehouse *et al.*, 1993). The coordination of Ti5 is comparable to that found for Ti^{4+} in the rutile structure. Thus, the ideal structure shows a clear crystal-chemical distinction between Ti1–Ti4 on one hand and Ti5 on the other. While the latter shows fairly regular

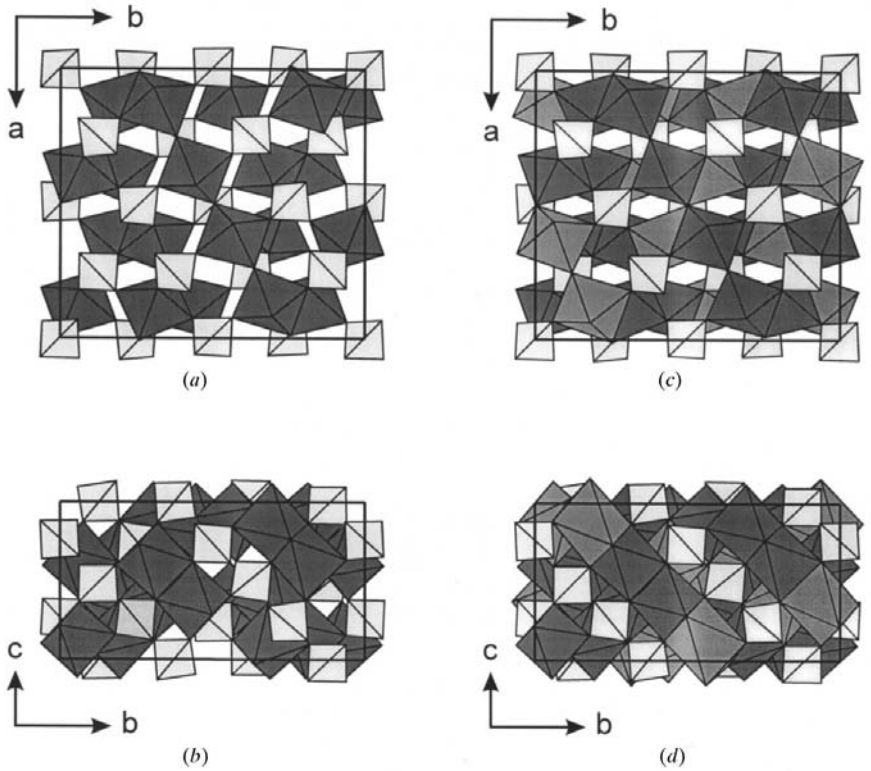

Fig. 6. $Ti_5O_4(PO_4)_4$. Projection of the ideal structure [model (I)] along (*a*) [001] and (*b*) [100]. Projection of the structure including Ti6, Ti7 and Ti8 along (*c*) [001] and (*d*) [100]. Light grey: PO_4; dark grey: TiO_6 containing Ti1–Ti5; medium grey: TiO_6 containing Ti6–Ti8. Plot produced with *ATOMS* (Dowty, 1995).

octahedral coordination with six similar d(Ti—O), the former reside within strongly distorted TiO_6 octahedra. These show the typical distance distribution for titanyl groups with one d(Ti—O) $\simeq$ 1.73 Å, four at intermediate distances and the sixth at d(Ti—O) > 2.15 Å.

It has to be pointed out that the disorder model used in our refinement [model (II)] is a rather simple one. It does not, for example, allow for positional shifts of Ti5 if the neighbouring positions Ti7 and/or Ti8 (*cf.* Fig. 5) are occupied. The significantly enlarged displacement ellipsoid of Ti5 along the 'chain' direction gives some evidence for this shortcoming of the model. In a similar way, one should expect for each of the eight Ti sites occupied in the real structure by titanium a splitting into three adjacent sites. Depending on the actual environment, Ti^{4+} could be sited (*a*) in an 'isolated' TiO_6 octahedron such as Ti5 in the ideal structure, (*b*) in the 'left' octahedron of a Ti_2O_9 dimer such as Ti2 and Ti4 or (*c*) in the 'right' octahedron of a Ti_2O_9 dimer such as Ti1 and Ti3 (for 'left' and 'right' see Fig. 5). Naturally, the disorder of Ti^{4+} in the real structure also affects the positions of the O atoms. Our structure refinement does not account for this effect. This is probably the reason for the rather high conventional residual R = 0.057. It can be easily seen that allowing for all deviations from the ideal atomic arrangement is far beyond the quality and significance of our data set.

The real structure of $\square_3Ti_5O_4(PO_4)_4$ is revealed by HRTEM investigations and accompanying model calculations of the observed image contrast. Several arrangements of the Ti^{4+} deviating from the ideal structure are observed. The resulting contrast variations in the HRTEM images can be matched well in simulation calculations by distributing Ti^{4+} over the eight sites of the real structure (Fig. 10).

Despite the cation disordering in $Ti_5O_4(PO_4)_4$, our investigations gave no evidence for a homogeneity range of the compound, according to partial reduction (*e.g.* substitution of three Ti^{4+} cations and one vacancy by four Ti^{3+} cations). Under slightly reducing conditions we have always obtained a new discrete phase of approximate composition $Ti^{3+}Ti_8^{4+}O_7(PO_4)_7$ (Reinauer *et al.*, 1994). Structural investigations of this compound, which has unit-cell dimensions related to $Ti_5O_4(PO_4)_4$, are in progress.

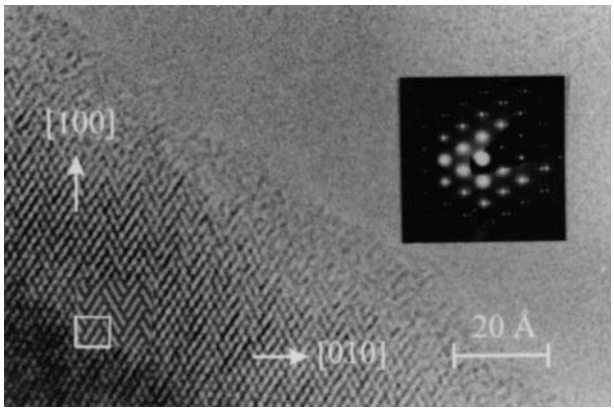

Fig. 7. HRTEM image of $Ti_5O_4(PO_4)_4$. Projection along [001]. The inset shows a simulation of the ideal structure [model (I)]. The unit cell is indicated by white lines.

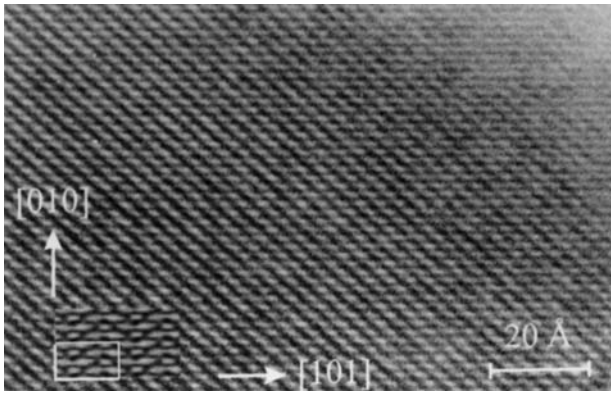

Fig. 8. HRTEM image of $Ti_5O_4(PO_4)_4$. Projection along [10$\bar{1}$]. The inset shows a simulation of the ideal structure [model (I)].

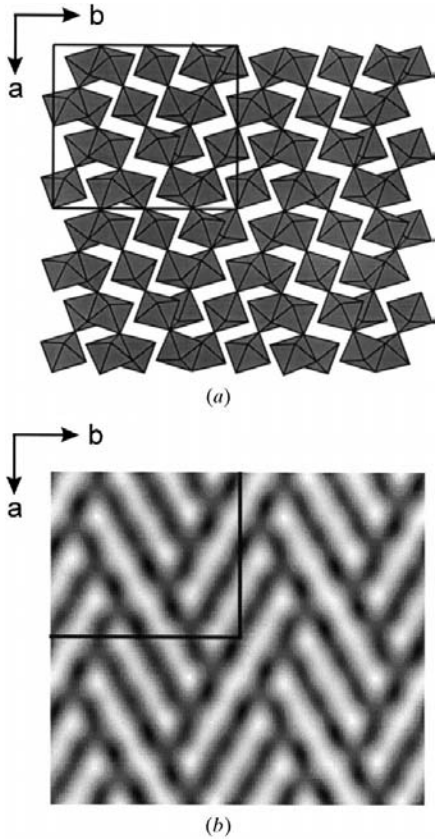

Fig. 9. Correlation of TiO_6 octahedra of (*a*) the crystal structure [model (I)] and (*b*) HRTEM image (projection along [001]) contrast simulation for $Ti_5O_4(PO_4)_4$. Unit cells in (*a*) and (*b*) are indicated by black lines.

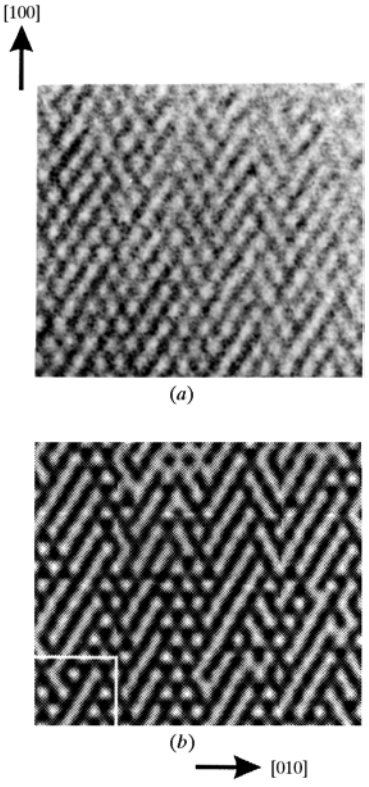

Fig. 10. Array of 4 × 4 unit cells of $Ti_5O_4(PO_4)_4$ showing deviations from the ideal distribution [model (I)] of Ti^{4+} over the octahedral voids. (*a*) HRTEM image (projection along [001]); (*b*) contrast simulation using *EMS* (Stadelmann, 1987).

The authors wish to thank Professor Dr R. Gruehn for stimulating discussions and continuous support. Thanks are also due to Professor Dr J. Beck for enlightening hints on group–subgroup relations and to G. Koch and T. Hilbert for the measuring and absorption correction of the X-ray data.

References

Bamberger, E. & Begun, G. M. (1987). *J. Less-Common Met.* **134**, 201–209.
Bärnighausen, H. (1980). *Match*, **9**, 139–175.
Bernardinelli, G. & Flack, H. D. (1985). *Acta Cryst.* A**41**, 500–511.
Brese, N. E. & O'Keeffe, M. (1991). *Acta Cryst.* B**47**, 192–197.
Dowty, E. (1995). *ATOMS for Windows*. Version 3.1. Shape Software, 521 Hidden Valley Road, Kingsport, TN 37663, USA.
Ech-Chahed, B., Jeannot, F., Malaman, B. & Gleitzer, C. (1988). *J. Solid State Chem.* **74**, 47–59.
Gatehouse, B. M., Platts, S. N. & Williams, T. B. (1993). *Acta Cryst.* B**49**, 428–435.
Glaum, R. & Gruehn, R. (1989). *Z. Kristallogr.* **186**, 91–93.
Glaum, R. & Schmidt, A. (1997). *Z. Anorg. Allg. Chem.* **623**, 1672–1678.
Golynko-Vol'fson, S. L. & Sudakas, L. G. (1966). *Izv. Akad. Nauk. SSSR*, **2**, 343.
Hagman, L.-O. & Kierkegaard, P. (1968). *Acta Chem. Scand.* **22**, 1822.
Harrison, D. E. & Hummel, F. A. (1959). *J. Am. Ceram. Soc.* **42**, 487.
Herrendorf, W. (1993). *HABITUS. Programm zur Optimierung der Kristallgestalt für die numerische Absorptionskorrektur anhand geeigneter φ-abgetasteter Reflexe*. PhD thesis, University of Karlsruhe, Germany.
Ijjaali, M., Malaman, B., Gleitzer, C., Warner, J. K., Hriljac, J. A. & Cheetham, A. K. (1990). *J. Solid State Chem.* **86**, 195–205.
Johnson, C. K. (1965). *ORTEP*. Report ORNL-3794. Oak Ridge National Laboratory, Tennessee, USA.
Levi, G. R. & Peyronel, G. (1935). *Z. Kristallogr.* **92**, 190–209.
Reinauer, F. (1998). PhD thesis, University of Giessen, Germany.
Reinauer, F., Glaum, R. & Gruehn, R. (1994). *Eur. J. Solid State Inorg. Chem.* **31**, 779–791.
Renninger, M. (1935). *Z. Phys.* **106**, 141–176.
Sheldrick, G. M. (1976). *SHELX*76. *Program for Crystal Structure Determination*. University of Cambridge, England.
Sheldrick, G. M. (1985). *SHELXS*86. *Program for the Solution of Crystal Structures*. University of Göttingen, Germany.
Sheldrick, G. M. (1990). *Acta Cryst.* A**46**, 467–473.
Sheldrick, G. M. (1993). *SHELXL*93. *Program for the Refinement of Crystal Structures*. University of Göttingen, Germany.
Stadelmann, P. A. (1987). *Ultramicroscopy*, **21**, 131–146.
Stucky, G. D., Eddy, M. M., Gier, Th. E., Keder, N. L., Cox, D. E., Bierlein, J. D. & Jones, G. (1988). *Inorg. Chem.* **27**, 1856–1858.
Tordjman, I., Masse, R. & Guitel, J. C. (1974). *Z. Kristallogr.* **103**, 139.
Vencato, I., Mattievich, E. & Primerano Mascarenhas, Y. (1989). *Am. Mineral.* **74**, 456–460.
Winkler, A. & Thilo, E. (1966). *Z. Anorg. Allg. Chem.* **346**, 492.